

Published in final edited form as:

Acta Biomater. 2010 September ; 6(9): 3729–3739. doi:10.1016/j.actbio.2010.03.021.

Biomimetic remineralization as a progressive dehydration mechanism of collagen matrices – implications in the aging of resin-dentin bonds

Young Kyung Kim^{a,*}, Sui Mai^{b,*}, Annalisa Mazzone^c, Yan Liu^d, Arzu Tezvergil-Mutluay^e, Kei Takahashi^f, Kai Zhang^b, David H. Pashley^g, and Franklin R. Tay^{g,h,**}

^a Department of Conservative Dentistry, School of Dentistry, Kyungpook National University, 2-188-1, Samduk-dong, Jung-gu, Daegu, Korea ^b Department of Operative Dentistry and Endodontics, Guanghua School of Stomatology, Sun Yat-sen University, 56 Lingyuanxi Rd., Guangzhou, China ^c Department of SAU&FAL, University of Bologna, Bologna, Italy ^d Department of Stomatology, Tongji Hospital, Huazhong University of Science and Technology, 1095 Jiefang Rd., Wuhan, China ^e Department of Prosthodontics, Institute of Dentistry, University of Turku, Lemminkaisenkatu 2, Turku, Finland ^f Department of Operative Dentistry, Okayama University, 2-5-1 Shikata-cho, Okayama, Japan ^g Department of Oral Biology, School of Dentistry, Medical College of Georgia, 1120 15th St., Augusta, GA, USA ^h Department of Endodontics, School of Dentistry, Medical College of Georgia, 1120 15th St., Augusta, GA, USA

Abstract

Biomaterialization is a dehydration process in which water from the intrafibrillar compartments of collagen fibrils are progressively replaced by apatites. As water is an important element that precipitates the lack of durability of resin-dentin bonds, this study examined the use of a biomimetic remineralization strategy as a progressive dehydration mechanism for preserving joint integrity and maintaining adhesive strength after aging. Human dentin surfaces were bonded with dentin adhesives, restored with resin composites and sectioned into sticks containing the adhesive joint. Experimental specimens were aged in a biomimetic analog-containing remineralizing medium and control specimens in simulated body fluid for up to 12 months. Specimens retrieved from the designated periods were examined by transmission electron microscopy for manifestation of water-rich regions using a silver tracer and for collagen degradation within the adhesive joints. Tensile testing was performed to determine the potential loss of bond integrity after aging. Control specimens exhibited severe collagen degradation within the adhesive joint after aging. Remineralized specimens exhibited progressive dehydration as manifested by silver tracer reduction and partial remineralization of water-filled micro-channels within the adhesive joint, as well as intrafibrillar remineralization of collagen fibrils that were demineralized initially as part of the bonding procedure. Biomimetic remineralization as a progressive dehydration mechanism of water-rich, resin-sparse collagen matrices enables those adhesive joints to resist degradation over the 12-month aging period, as verified by the conservation of their tensile bond strengths. The

**Corresponding Author: Department of Endodontics, School of Dentistry, Medical College of Georgia, 1120, 15th Street, CL 2132, Augusta, Georgia, 30912-1129, USA, Tel.: +1 706 721 2033; Fax: +1 706 721 6252; ftay@mcg.edu.

*These authors contributed equally to this work

Publisher's Disclaimer: This is a PDF file of an unedited manuscript that has been accepted for publication. As a service to our customers we are providing this early version of the manuscript. The manuscript will undergo copyediting, typesetting, and review of the resulting proof before it is published in its final citable form. Please note that during the production process errors may be discovered which could affect the content, and all legal disclaimers that apply to the journal pertain.

ability of the proof-of-concept biomimetic remineralization strategy to prevent bond degradation warrants further development of clinically-relevant delivery systems.

Keywords

Biomimetics; Dehydration; Intrafibrillar; Dentin adhesive; Remineralization

1. Introduction

Water, collagen and apatite are three primary components of mineralized dentin. In its unmineralized state, the collagen matrix contains up to 70% water by volume [1,2]. While most of this water exists as bulk free water, different categories of bound water bind with variable degrees of affinity to the triple helices of the collagen molecules and their interhelical polar side chains [3]. During mineralization, water provides the aqueous environment [4] for the infiltration of amorphous calcium phosphate precursors [5] into collagen fibrils to initiate nucleation and growth of intrafibrillar apatite crystallites in the gap zones of the collagen fibril. As mineralization proceeds, the loosely bound and bulk free water of the collagen matrix is progressively replaced by the intrafibrillar crystallites within the collagen fibrils and extrafibrillar apatite crystallites along the interfibrillar spaces [6–8]. The innermost hydration layer of tightly bound water cannot be removed without destroying the structural integrity of the collagen molecules [3,9]. Biomineralization is a progressive dehydration process; as the mineral content increases, the water content of the collagen matrix reciprocally decreases to maintain a constant volume, as recently demonstrated by nuclear magnetic resonance [10]. Thus, in mineralized dentin, 50 vol% of the dentin matrix is occupied by apatitic crystallites, 30 vol% by collagen and only 20 vol% is occupied by water [11]. The latter includes bulk free water that resides within the pore volume contributed by dentinal tubules and their anastomosing branches [12,13].

Any change in the mineral fraction of the collagen matrix is accompanied by a compensatory change in water fraction [10]. Dentin bonding with the use of etch-and-rinse adhesives is a unique form of tissue engineering in which dentists completely demineralize the surface 5–8 μm of the intertubular dentin matrix with phosphoric acid to create microspaces for infiltration of adhesive resin monomers for retention of tooth-colored fillings [14]. During this etch-and-rinse process, the entire mineral phase (50 vol%) is extracted and replaced by rinse-water which, when combined with the 20 vol% of intrinsic water, yields 70 vol% water and 30 vol% collagen. During the subsequent comonomer infiltration phase of resin bonding, this 70% water should ideally be completely replaced by the resin monomers that polymerize *in-situ* to produce a hybridized structural entity of resin and collagen known as the hybrid layer. However, due to the fluid movement within the dentinal tubule anastomosis complex during resin infiltration, often aggravated by the presence of positive pulpal pressure derived from a vital dental pulp, resin-water replacement is never ideal [15]. This results in incomplete infiltration of the water-filled collagen matrix by adhesive resins and the concomitant retention of water within the resin-infiltrated collagen matrix. Water derived from the dentinal tubules may also be trapped within the overlying adhesive layer due to convective and evaporative water movements during the solvent evaporation phase and the polymerization phase of adhesive application [16]. These water-rich, resin-sparse regions within the dentin hybrid layer and the polymerized adhesive layer may be identified with water-soluble tracers [17]. Water-rich domains have been estimated to be in the range of 2–3% of the volume of the hybrid layer when they are first created. However, the area occupied by the water-rich zones has been reported to increase with aging [18]. This phenomenon is attributed to the hydrolysis and dissolution of hydrophilic resin components from the adhesive, and degradation of the resin-

sparse collagen matrix by endogenous matrix metalloproteinases, with the residual water functioning as a medium for enzymatic action [15,16]. Irrespective of the cause, increase in tracer distribution within the hybrid layer signifies an augmentation of its water content. The corollary to the increase in tracer distribution is the reciprocal reduction in either the volume (*ca.* 67–68 vol%) of the resin component that is supposed to permanently replace the mineral component, or the natural scaffolding component (*i.e.* collagen network) of the tissue-engineered dentin.

Current *in vitro* and *in vivo* data indicate that dentin bonding is not as durable [15,16] as when the dentin hybridization concept was first proposed in the early 1980s. The lack of durability of resin-dentin bonding contributes, in part, to the high priority concern expressed in the National Institute of Dental and Craniofacial Research 2009–2013 Strategic Plan, that tooth-colored resin restorations have an average replacement time of 5.7 years due to secondary decay precipitated by bond failure [19].

Apatite-water replacement by progressive dehydration in natural biomineralization results in highly stable biocomposites, with the apatite protecting the organic matrix over millions of years [20]. The mineral component also precludes microbial extracellular enzymes from penetrating and deteriorating the collagen matrix during those lengthy aging periods [21]. Conversely, the resin-water replacement strategy as practiced in contemporary dentin bonding is incapable of dehydrating the collagen matrix sufficiently within the time frames (*ca.* 30 sec) in which the adhesives are applied [22]. Likewise, current attempts to extend the longevity of resin-dentin bonds via incorporation of more hydrolytically stable resin monomers [23] and/or the use of matrix metalloproteinase inhibitors [24] fail to address two fundamental issues that precipitate the degradation of resin-dentin bonds: dissolution of the mineral phase which exposes the collagen to biodegradation, and elimination of water from hybrid layers. After all, enzymatic action of matrix metalloproteinases cannot proceed in the absence of water as a functional medium.

A biomimetic remineralization strategy based on the use of polyanionic molecules to mimic the sequestering and templating functions of dentin noncollagenous proteins during the natural biomineralization process has been developed [25]. This particle-mediated, bottom-up mineralization approach [26,27] is different from conventional remineralization techniques currently employed in dentistry in two aspects. Firstly, it mimics the progressive dehydration mechanism of natural biomineralization by replacing the free and loosely bound water within a collagen matrix by apatite crystallites via the use of polyanion-stabilized amorphous calcium phosphate nanoprecursors. Decrease in water content in collagen matrices that are mineralized using a similar polymer-induced liquid precursor of amorphous calcium carbonate has been confirmed using magnetic resonance microscopy [28]. Secondly, biomimetic mineralization via a bottom-up particle assembly approach proceeds in the absence of apatite seed crystallites in a collagen matrix [29]. Whereas epitaxial growth on seed crystallites is a thermodynamically more favorable process [30], mineralization in the absence of seed crystallites requires alternative kinetically-driven protein/polymer-modulated pathways for lowering the activation energy barrier for crystal nucleation via sequential steps of phase transformations, as depicted by nonclassical crystallization theory [30,31]. Intrafibrillar mineralization of collagen fibrils by apatite crystallites has been shown to occur in acid-etched dentin that are completely devoid of seed crystallites using this biomimetic remineralization strategy [25,32].

Inasmuch as there is no available mechanism to dehydrate the remnant water within the hybrid layer after adhesive application, a biomimetic remineralization strategy that mimics the progressive dehydration mechanism during hard tissue mineralization appears to be a rational approach for remineralizing water-rich, resin-sparse regions within hybrid layers.

Such a mechanism has been shown to be viable in studies that involved short-term remineralization of hybrid layers created by different dentin adhesives [32–35]. What is not known, however, is whether biomimetic remineralization of hybrid layers can result in improving the durability of resin-dentin bonds after aging. Hence, the objective of this long-term study was to investigate the feasibility of biomimetic remineralization of hybrid layers as a means to improve the longevity of resin-dentin bonds. The present aging study utilized a proof-of-concept lateral diffusion approach as the means of remineralization of hybrid layers, prior to the adoption of more sophisticated designs for translation of this approach into clinically-applicable schemes. As biomimetic remineralization is a progressive dehydration process, increase in minerals in the water-rich, resin-sparse regions of the hybrid layer should be accompanied by a reduction in water content [10,31], which in turn, should result in a decrease in the distribution of a water-soluble tracer. Thus, the first null hypothesis tested was that there is no difference in the distribution of silver tracers in hybrid layers aged for 12 months that are stored in a biomimetic remineralization medium versus those that are stored in a non-remineralizing medium. Theoretically, reduction of water by progressive dehydration should increase the longevity of resin-dentin bonds, as water becomes less readily available for the functioning of the collagen degrading enzymes. Moreover, these host-derived collagen-bound enzymes [36] may be fossilized by the intrafibrillar crystallites that are deposited within and on the collagen fibrils [20]. Thus, the second null hypothesis tested was that there is no difference in the ability of specimens aged for 12 months in a biomimetic remineralization medium versus those aged in a non-remineralizing medium in their ability to resist the degradation of resin-dentin bonds.

2. Materials and Methods

2.1 Sustained releasing source of calcium and hydroxyl ions

Set white Portland cement (Lehigh Cement Company, Allentown, Pennsylvania, USA) was used as a sustained releasing source of calcium and hydroxyl ions for the remineralization process. The cement was mixed with deionized water in a 0.35:1 water-to-powder ratio and allowed to set and aged at 100% relative humidity for one week before use.

2.2 Phosphate source and biomimetic molecules

The biomimetic remineralization strategy employed in the present study was based on the use of polyanionic molecules published in our previous studies [32–35]. A simulated body fluid (SBF) was prepared by dissolving 136.8 mM NaCl, 4.2 mM NaHCO₃, 3.0 mM KCl, 1.0 mM K₂HPO₄·3H₂O, 1.5 mM MgCl₂·6H₂O, 2.5 mM CaCl₂ and 0.5 mM Na₂SO₄ in deionized water and adding 3.08 mM sodium azide to prevent bacterial growth. The SBF was buffered to pH 7.4 with 0.1 M Tris Base and 0.1 M HCl and filtered through a 0.22 μm Millipore filter. The SBF was used as the immersion medium for the control groups. For the biomimetic remineralization groups, a proprietary polyanion cocktail of polycarboxylic and polyphosphonic acids in the range of 200–1,000 ppm (Shandong Taihe Water Treatment Co. Ltd., Shandong, China) were pre-packaged in gelatin capsules. One capsule was added on demand to the SBF under nitrogen to minimize CO₂ adsorption. The pH of the remineralization medium was adjusted to 7.4. The latter was kept frozen at –70°C until use.

2.3 Dentin bonding

One hundred and forty-four recently extracted noncarious human third molars were collected after receiving the patients' informed consent under a protocol approved by the MCG Human Assurance Committee. Seventy-two teeth were randomly assigned to one of the two unfilled, etch-and-rinse adhesives: One-Step (Bisco Inc., Schamburg, IL, USA), an acetone-based adhesive, and Single Bond (3M ESPE, St. Paul, MN, USA), an ethanol-based adhesive. A flat dentin surface was prepared perpendicular to the longitudinal axis of each

tooth using a slow-speed Isomet diamond saw (Buehler Ltd, Lake Bluff, IL, USA) under water-cooling. The occlusal dentin surface was polished with a 400-grit silicon carbide paper under running water to create a bonding surface in mid-coronal dentin. Each dentin surface was etched with a 32% phosphoric acid gel for 15 sec to create a 5–8 μm thick zone of completely demineralized dentin on top of a mineralized dentin base. The etched dentin surface was thoroughly rinsed with deionized water and bonded with the respective adhesive by keeping the etched dentin visibly moist during bonding. After evaporation of the adhesive solvent, each adhesive was polymerized for 20 sec using a quartz-tungsten-halogen light-curing unit. This was followed by incremental placement of two 2-mm thick layers of a resin composite that was light-cured separately for 40 sec.

After storage in deionized water at 37°C for 24 h, each tooth was vertically sectioned into 0.9 mm thick composite-dentin slabs, with the adhesive joint in the middle of each slab. The four central slabs of each tooth were sectioned into 0.9 \times 0.9 mm sticks, each containing the adhesive joint in the center of the stick. The two longest sticks from each slab were selected, yielding 8 sticks per tooth. The 576 sticks derived from the 72 teeth of each adhesive were pooled together and then randomly assigned to either the control group (288 sticks) or the biomimetic remineralization group (288 sticks).

2.4 Biomimetic remineralization

For the biomimetic remineralization group of each adhesive, four composite-dentin sticks were random chosen and placed on top of a set Portland cement block (*ca.* 1 g) inside a glass scintillation vial (total 144 vials). Each vial was filled with 15 mL of the biomimetic remineralization medium, capped and incubated at 37°C. The medium was changed every month for up to 12 months. The pH of the medium inside the vials was monitored weekly to insure that they were above 9.25. This ensured that apatite was formed instead of octacalcium phosphate [37].

For the control group of each adhesive, four composite-dentin sticks were randomly selected and placed inside a scintillation vial (total 144 vials) containing 15 mL of SBF and incubated at 37°C. The medium was also changed every month for up to 12 months.

2.5 Transmission electron microscopy before and after different aging periods

Six aging periods were designated for the control and remineralization groups of each adhesive: 24 h (baseline), 1 month, 2 months, 3 months, 6 months and 12 months. Two vials (*i.e.* 8 sticks) were retrieved from the control group and two vials from the remineralization group of each adhesive at each designated aging period. For each group, six sticks were examined using a silver tracer protocol to determine the potential water-filled regions within the resin-dentin interfaces [38]. The sticks were immersed in a 50 wt% aqueous ammoniacal AgNO_3 tracer solution for 48 h. They were then rinsed with deionized water for 30 min, placed in a photodeveloping solution for 8 hours under fluorescent light to reduce the diamine silver ions ($[\text{Ag}(\text{NH}_3)_2]^+$) into metallic silver grains within the water-filled, resin-sparse regions of the hybrid layer. Thereafter, the silver-impregnated sticks were processed for transmission electron microscopy (TEM). The sticks were fixed in Karnovsky's fixative and post-fixed in 1% osmium tetroxide. They were then dehydrated in an ascending ethanol series (50–100%), immersed in propylene oxide and embedded in epoxy resin. Non-demineralized, 90 nm thick sections were prepared and examined without further staining using the JEM-1230 TEM (JEOL, Tokyo, Japan) at 110 kV.

To examine the conditions of the collagen matrix after aging, the other two sticks from the respective control and remineralization groups of each adhesive were completely demineralized in a formic acid/sodium formate buffer for 10 days. These demineralized

specimens were fixed and embedded in epoxy resin in the manner described previously. Ninety nanometer thick sections were double-stained with 2% methanolic uranyl acetate and aqueous lead citrate prior to TEM examination. In addition, for the 12-month aged remineralized groups only, non-demineralized TEM sections that demonstrated extensive remineralization were demineralized in-situ to confirm the absence of degradation of the collagen matrix. This procedure was not performed for the 12-month aged control groups as the procedure precluded high resolution examination of the degradation elements within the degraded hybrid layers. Each carbon and formvar-coated nickel grid containing the mineralized section was placed upside down over a group of 0.1 N HCl for 30 sec. The demineralized sections were then rinsed with deionized water, double-stained with uranyl acetate and lead citrate for TEM re-examination.

2.6 Tensile strength testing

At each of the six designated aging periods, 10 vials (i.e. 40 sticks) were taken from the control group and 10 vials from the remineralized group of each adhesive for tensile testing. The rationale for performing tensile testing was to identify if there was a loss in strength of the adhesive joint after water aging. A well-reported microtensile bond strength evaluation technique was adopted [39]. Each stick was stressed to failure under tension using a Vitrodyne V1000 universal tester (Liveco Inc, Burlington, VT, USA) at a cross-head speed of 1 mm/min. Each stick was used as the unit for statistical analysis (N = 40). Data from the two adhesives were analyzed separately. As the normality (Kolmogorow-Smirnoff test) and homoscedasticity assumptions (Levene test) of the data appeared to be valid, they were analyzed using two-way repeated ANOVA, with aging method (i.e. control vs. remineralization) as one factor and the aging period as the repeating factor. Post-hoc comparisons were performed with the Tukey test. Statistical significance were set at $\alpha = 0.05$. Representative separated beams from the control and remineralized groups with bond strengths close to the mean bond strength of that group were air-dried and sputter-coated with gold/palladium for examination of the failure modes using a field-emission scanning electron microscope (FE-SEM; XL-30 FEG; Philips, Eindhoven, The Netherlands) at 5 keV. Failure modes were classified as adhesive (i.e. interfacial), cohesive (i.e. within composite or dentin) or mixed failures.

3. Results

Representative examples of 12-month aged resin-dentin interfaces of One-Step and Single Bond are illustrated in Figures 1 and 2, respectively. Hybrid layers in the control specimens that had been aged in SBF for 12 months contained regions with bulk silver deposits when those specimens were immersed in the tracer solution prior to laboratory specimen processing (Figs. 1a, 2a). Examination of laboratory demineralized control specimens from the same aged period indicate that those water-filled spaces represent areas of extensive degradation of collagen matrices within the hybrid layers (Figs. 1b, 2b). At high magnifications, unraveling of collagen fibrils were seen adjacent to the bottom of the superficial intact hybrid layers, as well as the junction between the base of the degraded hybrid layers and the underlying intact dentin. In the center region of those degraded hybrid layers, the grossly unraveled fibrils were further denatured into segregated microfibrillar strands (not shown). Conversely, hybrid layers in experimental specimens that had been aged in the biomimetic remineralization medium for 12 months show regions with extensive remineralization (Figs. 1c, 2c). Those remineralized regions (Figs. 1c, 2c) correspond with the locations of bulk silver deposits (Figs. 1a, 2a) and degraded hybrid layers (Figs. 1b, 2b) in the control specimens. *In-situ* demineralization of sections from the experimental groups with confirmed remineralization revealed intact collagen matrices within the remineralized hybrid layers (Figs. 1d, 2d).

Progressive dehydration of water-containing spaces within the hybrid layers before and after various periods of remineralization is depicted by the reduction in the complexity in which the patterns of silver tracer were expressed. This is illustrated in Figures 3 for One-Step and Figure 4 for Single Bond. A characteristic baseline reticular silver tracer pattern within the hybrid layer created by One-Step (Fig. 3a) or Single Bond (Fig. 4a) consists of silver clusters that ramify from a silver-impregnated micro-branching of dentinal tubules. Figure 3b depicts an early stage of remineralization of the hybrid layer created by the One-Step adhesive. There was a reduction of the silver cluster ramifications and only remnants of the larger silver-impregnated micro-branches were present. The latter, illustrated in higher magnifications in Fig. 3c, are 200 nm diameter channels that led to 100 nm diameter side branches and terminal knob-like structures. In addition, small silver grains with a gradient of decreasing dimensions could be seen extending from the silver-impregnated water-filled channel to the adjacent partially-remineralized, resin-infiltrated collagen matrix. Figure 3d represents an intermediate stage of remineralization that consists predominantly of intrafibrillar remineralization of the collagen fibrils. The interfibrillar spaces (*ca.* 20–30 nm wide) were not remineralized as they were filled by the polymerized adhesive resins. Cross sections of silver-impregnated water-filled channels (*ca.* 200 nm wide) could be seen within the hybrid layer.

Figures 4b–4d are representative of an advanced stage of biomimetic remineralization of hybrid layers created by Single Bond. Silver-impregnated micro-channels were only sparsely identified in the remineralized hybrid layer at this advanced stage of remineralization (Fig. 4b). Only isolated silver grains, representing water-rich domains of the hydrophilic resin matrix [42], could be seen in the adhesive layer (Fig. 4c) and the remineralized hybrid layer (Fig. 4d).

Figure 5 represents progressive dehydration of the water-filled channels trapped within the adhesive from water that evaporated from the dentinal tubules during bonding procedures. During the early stage of remineralization, silver deposits were abundantly seen within these obliquely oriented water-filled channels (Fig. 5a). The bulk silver deposits were scattered among the parallel arrays of nanocrystals (*ca.* 20 nm in length) that were deposited as a result of biomimetic remineralization (Fig. 5b). Selected area electron diffraction of those nanocrystals yielded concentric ring patterns that are characteristic of polycrystalline apatite (not shown). As remineralization proceeded to a more advanced stage, both the large silver-impregnated micro-channels in the hybrid layer and silver deposits within the water-filled channels entrapped within the adhesive were considerably reduced (Fig. 5c). A high magnification of a water-filled channel in the adhesive layer that was completely filled with apatite nanocrystals is shown in Fig. 5d. Bulk silver deposits were completely absent and only scattered isolated silver grains could be identified.

Changes in microtensile bond strengths with increasing aging time for dentin specimens bonded with the two adhesives are shown in Table I. For each adhesive, both the aging method (*i.e.* control *vs.* remineralization; $p < 0.001$) and the repeated aging factor (baseline, 1, 2, 3, 6 and 12 months; $p < 0.001$) significantly affected the bond strength results. Significant interactions between the two factors were also observed for both adhesives ($p < 0.001$), with the effect of aging method dependent upon the level of aging. For both adhesives, significant decline in tensile bond strengths in the control group occurred after 2–3 months of aging in SBF ($p < 0.05$). Conversely, there was no significant drop in tensile bond strengths for both adhesives throughout the entire 12-month aging period when the bonded specimens were aged in the biomimetic remineralization medium ($p > 0.05$). For One-Step, significant differences between the control and remineralized groups occurred after the first month (*i.e.* 2, 3, 6 and 12 months, $p < 0.05$ for each post-hoc comparison). For

Single Bond, significant differences between the control and remineralized groups occurred after the second month (i.e. 3, 6 and 12 months, $p < 0.05$ for each post-hoc comparison).

Failure modes of the resin-dentin beams at any time period demonstrated predominantly mixed failure modes. At the SEM level, pure interfacial failure and cohesive failure in the mineralized dentin was never observed. Also, it was not possible to differentiate between specimens bonded by the two adhesives. As the fracture modes for the two adhesives were similar, the description below is representative of both adhesives. An example of a separated dentin in the control group after 12 months of aging typically revealed a mixed failure mode in dentin and adhesive (Fig. 6a). At high magnification, denuded collagen fibrils could be observed at the base of the fractured hybrid layer but there were also regions that were completely devoid of collagen fibrils and with the mineralized dentin based exposed (Fig. 6b). An example of a separated dentin in the remineralized group after 12 months of aging typically revealed a mixed failure mode in composite and adhesive, with partial interfacial failure along the dentin surface (Figs. 6c, 6d).

4. DISCUSSION

The ultrastructural results of the present study indicate that there was progressive reduction in the amount of silver tracer uptake over time and hence the degree of water distribution in resin-dentin interfaces that had been subjected to biomimetic remineralization. Conversely, a dramatic increase in silver tracer deposits was observed when collagen-rich, resin-sparse regions of the hybrid layers degraded and became replaced by water in control specimens that had been aged only in SBF. Thus, the first null hypothesis that there is no difference in the distribution of silver tracers in aged hybrid layers that are stored in a biomimetic remineralization medium versus those that are stored in a non-remineralizing medium has to be rejected. As decline in tensile bond strengths occurred only in aged specimens that had not been subjected to biomimetic remineralization, we have to reject the second null hypothesis tested that there is no difference in the ability of specimens aged in a biomimetic remineralization medium versus those aged in a non-remineralizing medium in their ability to resist the degradation of resin-dentin bonds.

A critical observation in the present study is the discrepancy between what was identified by the silver tracer as water-rich regions in the hybrid layers and the locations in which remineralization occurred in remineralized hybrid layers. Specifically, areas with subsequent extensive intrafibrillar remineralization could not be identified initially from baseline specimens by the silver tracer. This indicates the silver tracer method which has been widely employed in adhesive dentistry for the past 15 years underestimates the retention of water within apparently well-infiltrated collagen matrices in hybrid layers after bonding with etch-and-rinse and self-etch adhesives. Water must be present within the intrafibrillar spaces of those collagen networks before it can be displaced by fluidic amorphous nanoprecursors that are subsequently converted into intrafibrillar minerals [40]. There is a threshold with respect to the size of molecules that can penetrate the intrafibrillar water compartments of type I collagen fibrils [8]. Small molecules such as glucose (180 Da) can diffuse into internal water compartments of a collagen fibril while molecules larger than 6 kDa (e.g. albumin, 6.6 kDa) are excluded from the fibril [8]. The small molecular mass of the ammoniacal silver ion complex ($[\text{Ag}(\text{NH}_3)_2]^+$) (67 Da) should not have restricted it from reaching the intrafibrillar water compartments of the collagen fibril. A possible explanation is that the water that remains within the collagen fibrils is bound water that is inaccessible to the ammoniacal silver ion complex. Conversely, the multiple negative charges present in the templating polyanionic biomimetic molecules could have competed with water for hydrogen bonding with the collagen molecules, freeing the water molecules and binding themselves non-specifically to the collagen molecules via electrostatic interactions. This probably explains

why the loosely bound water within the collagen fibrils is not displaced by the ammoniacal silver ion complex or the resin monomers that are used for bonding to dentin.

Assuming that the silver tracer is capable only of locating bulk free water within the micro-branches of the dentinal tubules, their side and terminal branches, and those interfibrillar spaces that are not infiltrated by adhesive resins, the reduction in complexity of the silver tracer distribution after biomimetic remineralization is remarkable. This suggests that apart from displacing water from the intrafibrillar components of the collagen fibrils, biomimetic remineralization also contributes to dehydration of some of the spaces occupied by bulk free water within the hybrid layer. As those spaces are devoid of a scaffolding component, displacement of water must have occurred at the expense of the deposition of an array of nanocrystals within those micro-channels, in a manner analogous to how the larger water-filled channels in the adhesive layer were progressively filled by nanocrystals. Figure 7 represents a schematic of how the bulk water-filled spaces within the hybrid layer are progressively reduced by the process of biomimetic remineralization, using an unmodified, negative-stained TEM image of the demineralized dentin collagen matrix as a template (Fig. 7A). The latter, because of its high contrast, demonstrates nicely the continuum between the micro-branches of the dentinal tubule anastomosis complex, their side branches and the interfibrillar spaces of the collagen fibrils. The dimensions of these spaces are comparable to the pore dimensions reported recently in demineralized dentin using mercury intrusion porosimetry [13]. In that study, a bimodal pore size distribution was observed, with those in the 1 μm range corresponding to the dentinal tubules and their lateral branches and those in the 1–100 nm range corresponding to the micro-branches and the interfibrillar spaces. Prior to remineralization, the silver tracing depicts a reticular pattern of silver deposits that represent the bulk water-filled extrafibrillar spaces within the hybrid layer (Fig. 7B). The collagen fibrils may be sparsely coated by adhesive resin but the resin does not infiltrate the intrafibrillar compartments of those fibrils, which retain bound and free water. As biomimetic remineralization proceeds, phosphate-containing polyanionic acid molecules that bind non-specifically to the collagen fibrils act as templates for guiding the spatial arrangement of sequestered amorphous calcium phosphate nanoprecursors that penetrate the intrafibrillar compartments of the collagen fibrils. Free and loosely bound water is displaced from the fibrils as the amorphous nanophases are converted into intrafibrillar mineral crystallites. Dehydration may also occur as nanocrystals are deposited within interfibrillar spaces that are not occupied by resin, as well as from very small water-filled terminal branches of the dentinal tubule (Fig. 7c). With a more advanced stage of biomimetic remineralization, bulk water is further displaced from the extrafibrillar spaces (Fig. 7d). As the considerably larger micro-branches of the dentinal tubules are unlikely to be completely occluded by nanocrystals, free water may remain within these channels. This gives rise to the appearance of larger silver tracer deposits in a partially-remineralized hybrid layer. Completely elimination of all silver deposits was rarely observed. This is not unusual and simply represents how the micro-branches of the dentinal tubules in normal mineralized dentin are filled with bulk free water, or dentinal fluid in the case of vital dentin. As long as the collagen fibrils are filled with intrafibrillar apatite, they should be protected from degradation.

For more than a decade, the question remained unresolved as to whether dentin adhesives are capable of infiltrating the intrafibrillar spaces of collagen fibrils to form a continuum with those resins that occupy the extrafibrillar spaces [11]. The observation of intrafibrillar remineralization provides indirect evidence that dentin adhesives employed in the manner in which they are advocated by the manufacturers (i.e. bonding to a water-saturated demineralized dentin) cannot infiltrate the intrafibrillar compartments of the collagen fibrils. Although only etch-and-rinse adhesives were examined in this study, intrafibrillar remineralization was also evident in dentin bonded with self-etch adhesives [34,35] that are

supposed to demineralize and infiltrate collagen fibrils simultaneously. The Achilles' heel of contemporary dentin adhesives, at least in the manner in which they are applied to a water-saturated collagen matrix or in the presence of water as a co-solvent to facilitate ionization of acidic resin monomers, is their inability to replace water from the intrafibrillar compartments of the collagen fibrils. In principle, this is a poor form of tissue engineering with a heavy price to be paid - degradation of the natural scaffolding component. Collagen degradation within hybrid layers may be prevented by the use of matrix metalloproteinase inhibitors such as chlorhexidine [16]. However, progressive removal of water by intrafibrillar remineralization is a more proactive strategy if it can be translated into a clinically application scheme, as it addresses the fundamental issue of replacing mineral that was iatrogenically depleted from the intrafibrillar compartments of the collagen matrix during the acid-etching phase of dentin bonding. This should lead to a more durable form of tissue-engineered dentin that is capable of preserving or fossilizing its organic components, including the collagen-bound matrix metalloproteinases [20]. Preliminary three-point bending [32] and nanodynamic mechanical analysis (Tay and Arola, unpublished results) indicate that biomimetic remineralization of hybrid layers is capable of restoring the mechanical properties of water-sorbed hybrid layers. This probably accounts for the conservation of tensile strength in specimens that were aged in the biomimetic remineralization medium in the present study. Understandably, the stiffness of remineralized hybrid layers cannot be compared with natural mineralized dentin as the adhesive resins used for infiltrating the collagen matrices are much more viscoplastic than bioapatites.

Progressive dehydration of collagen matrices after dentin bonding with the experimental biomimetic remineralization protocol is similar to the experimental "ethanol wet bonding" technique [22] in that both encompass the philosophy of water depletion from intrafibrillar water compartments as the means of resisting degradation of resin-dentin bonds [41]. Whereas the former involves post-bonding replacement of intrafibrillar water by bioapatites, the latter involves replacement of intrafibrillar water during bonding with adhesive resins, with the ethanol providing the medium for small molecular size resin monomers such as BisGMA (512 Da) to enter the intrafibrillar spaces [42]. In the "ethanol wet bonding" technique, water from the demineralized collagen matrix is completely replaced by absolute ethanol prior to the application of water-free dentin adhesives. Provided that the technique is executed meticulously, no intrafibrillar remineralization is observed after the ethanol wet-bonded specimens are subjected to biomimetic remineralization. However, any slight water contamination during the application of the "ethanol wet bonding" technique results in localized intrafibrillar remineralization [42]. By contrast, biomimetic remineralization of dentin hybrid layers, as in natural biomineralization processes that involves amorphous calcium carbonate, is accomplished entirely in an aqueous medium at ambient temperature via liquid-liquid phase separation of fluidic polymer-stabilized amorphous nanophases from the water phase [43]. Liquid-liquid phase separation has not been reported between water and water-soluble hydrophilic resin monomers that are used in dentin adhesives. As hydrophobic resin components employed in dentin adhesives are immiscible with water, they undergo phase separation after evaporation of the adhesive solvent [44] and produce resin droplets in the presence of large water-resin molar ratios. Because of their hydrophobic nature, it is not possible for those resin droplets to replace water from the intrafibrillar compartments of the collagen fibrils.

It is important to stress that protease inhibitors were not included in the biomimetic remineralization medium to prevent degradation of hybrid layers that might occur before completion of the biomimetic remineralization process. This is because the polyphosphonic acid analog included in the medium serves the dual functions of a collagen-binding amorphous calcium phosphate nucleator and an inhibitor of matrix metalloproteinase (Tezvergil-Mutluay and Pashley, unpublished results). Organophosphonic acids are good

chelators of divalent and trivalent metal ions and are widely used as anti-scaling agents and corrosion inhibitors. Their corrosion inhibition efficiencies are increased when they are used in combination with zinc ions, producing zinc phosphonate complexes [45]. The ability to chelate zinc ions effectively may explain why polyphosphonic acids are effective inhibitors of matrix metalloproteinases, being zinc-dependent peptidases.

5. Conclusion

In the present study, we have demonstrated that incorporation of biomimetic analogs in a remineralization medium produces progressive dehydration of the remnant water residing in adhesive joints created by dentin adhesives. Dehydration is manifested by intrafibrillar remineralization of the collagen fibrils as well as reduction of the silver tracer used to identify bulk free water within micro-water-filled channels of resin-dentin interfaces. Biomimetic remineralization as a progressive dehydration mechanism of water-rich, resin-sparse collagen matrices enables those adhesive joints to resist degradation over a 12-month aging period, as verified by the conservation of their tensile bond strengths. The success of the current proof-of-concept, laterally-diffusing remineralization protocol in resisting the degradation of resin-dentin bonds warrants the development of a clinically-applicable delivery system by incorporating these biomimetic analogs into the steps involved in the application of these adhesives and filling materials.

Acknowledgments

This study was supported by Grant R21 DE019213-01 from the National Institute of Dental and Craniofacial Research (PI. Franklin R. Tay). We thank Michelle Barnes for secretarial support.

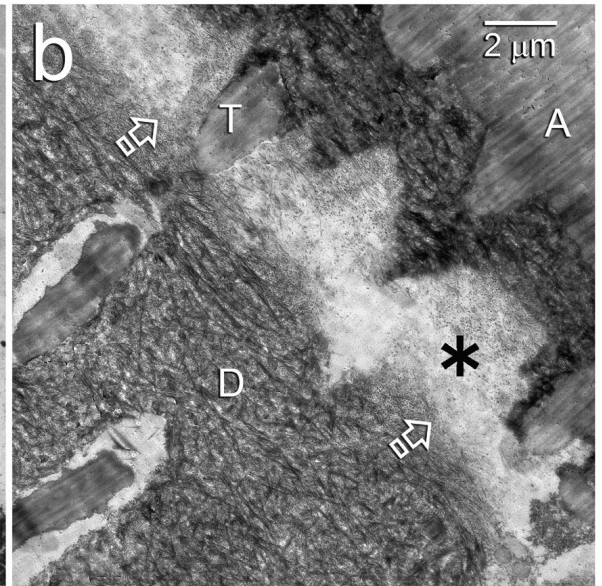
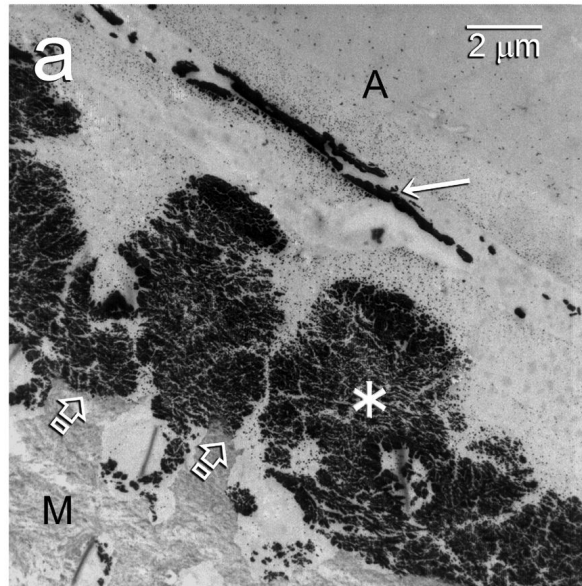
References

1. Shinyashiki N, Asaka N, Mashimo S, Yagihara S, Sasaki N. Microwave dielectric study on hydration of moist collagen. *Biopolymers* 1990;29:1185–1191. [PubMed: 2369631]
2. Fullerton GD, Amurao MR. Evidence that collagen and tendon have monolayer water coverage in the native state. *Cell Biol Int* 2006;30:56–65. [PubMed: 16488837]
3. Cameron IL, Short NJ, Fullerton GD. Verification of simple hydration/dehydration methods to characterize multiple water compartments on tendon type 1 collagen. *Cell Biol Int* 2007;31:531–539. [PubMed: 17363297]
4. Utku FS, Klein E, Saybasili H, Yucesoy CA, Weiner S. Probing the role of water in lamellar bone by dehydration in the environmental scanning electron microscope. *J Struct Biol* 2008;162:361–367. [PubMed: 18440829]
5. Mahamid J, Sharir A, Addadi L, Weiner S. Amorphous calcium phosphate is a major component of the forming fin bones of zebrafish: Indications for an amorphous precursor phase. *Proc Natl Acad Sci USA* 2008;105:12748–12753. [PubMed: 18753619]
6. Elliott SR, Robinson RA. The water content of bone. I. The mass of water, inorganic crystals, organic matrix, and CO₂ space components in a unit volume of the dog bone. *J Bone Joint Surg Am* 1957;39-A:167–188. [PubMed: 13385272]
7. Magne D, Weiss P, Bouler JM, Laboux O, Daculsi G. Study of the maturation of the organic (type I collagen) and mineral (nonstoichiometric apatite) constituents of a calcified tissue (dentin) as a function of location: a Fourier transform infrared microspectroscopic investigation. *J Bone Miner Res* 2001;16:750–757. [PubMed: 11316003]
8. Toroian D, Lim JE, Price PA. The size exclusion characteristics of type I collagen: implications for the role of noncollagenous bone constituents in mineralization. *J Biol Chem* 2007;282:22437–22447. [PubMed: 17562713]
9. De Simone A, Vitagliano L, Berisio R. Role of hydration in collagen triple helix stabilization. *Biochem Biophys Res Commun* 2008;372:121–125. [PubMed: 18485893]

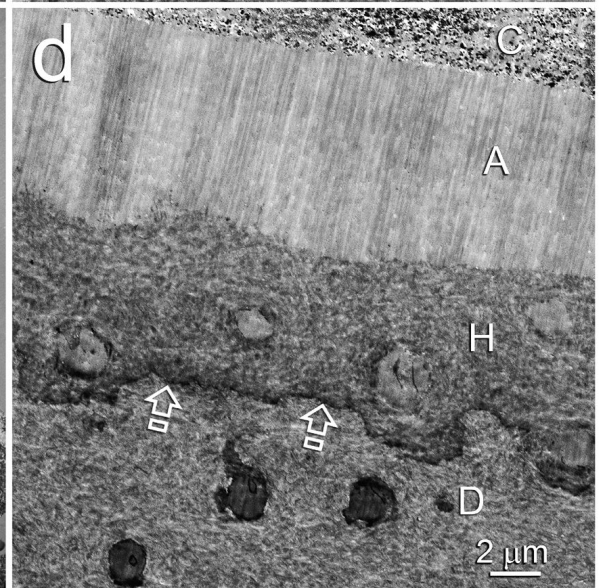
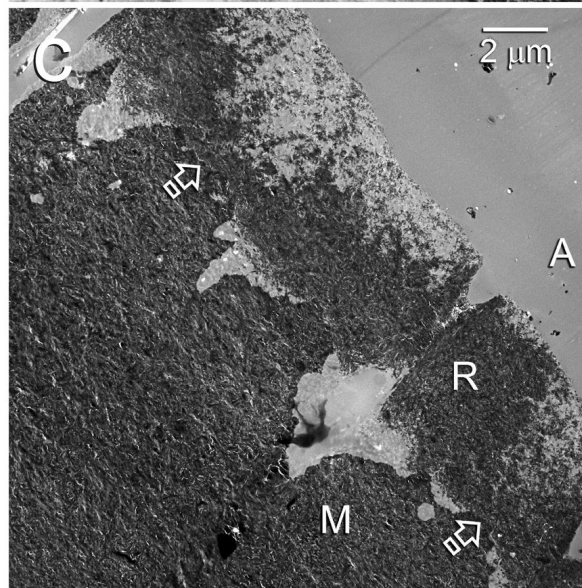
10. Wehrli FW, Fernández-Seara MA. Nuclear magnetic resonance studies of bone water. *Ann Biomed Eng* 2005;33:79–86. [PubMed: 15709708]
11. Nakabayashi, N.; Pashley, DH. Hybridization of dental hard tissues. Vol. 21. Quintessence Publishing Co. Ltd; Tokyo: 1998. p. 66
12. Mjör IA, Nordahl I. The density and branching of dentinal tubules in human teeth. *Arch Oral Biol* 1996;41:401–412. [PubMed: 8809302]
13. Vennat E, Bogicevic C, Fleureau JM, Degrange M. Demineralized dentin 3D porosity and pore size distribution using mercury porosimetry. *Dent Mater* 2009;25:729–735. [PubMed: 19174308]
14. Vaidyanathan TK, Vaidyanathan J. Recent advances in the theory and mechanism of adhesive resin bonding to dentin: a critical review. *J Biomed Mater Res B Appl Biomater* 2009;88:558–578. [PubMed: 18975378]
15. Hashimoto M. A Review-Micromorphological evidence of degradation in resin-dentin bonds and potential preventional solutions. *J Biomed Mater Res B Appl Biomater* 2009;92B:268–280.
16. Breschi L, Mazzoni A, Ruggeri A, Cadenaro M, Di Lenarda R, De Stefano Dorigo E. Dental adhesion review: aging and stability of the bonded interface. *Dent Mater* 2008;24:90–101. [PubMed: 17442386]
17. Sano H, Yoshiyama M, Ebisu S, Burrow MF, Takatsu T, Ciucchi B, et al. Comparative SEM and TEM observations of nanoleakage within the hybrid layer. *Oper Dent* 1995;20:160–167. [PubMed: 8700785]
18. Reis A, Grande RH, Oliveira GM, Lopes GC, Loguercio AD. A 2-year evaluation of moisture on microtensile bond strength and nanoleakage. *Dent Mater* 2007;23:862–870. [PubMed: 16950505]
19. NIDCR Strategic Plan 2009–2013.
<http://www.nidcr.nih.gov/Research/ResearchPriorities/StrategicPlan>
20. Collins MJ, Nielsen-Marsh CM, Hiller J, Smith CI, Roberts JP, Prigodich RV, Weiss TJ, et al. The survival of organic matter in bone: a review. *Archaeometry* 2002;44:383–394.
21. Child AM. Towards an understanding of the decomposition of bone in the archaeological environment. *J Archaeol Sci* 1995;22:165–174.
22. Pashley DH, Tay FR, Carvalho RM, Rueggeberg FA, Agee KA, Carrilho M, Donnelly A, et al. From dry bonding to water-wet bonding to ethanol-wet bonding. A review of the interactions between dentin matrix and solvated resins using a macromodel of the hybrid layer. *Am J Dent* 2007;20:7–20. [PubMed: 17380802]
23. Moszner N, Salz U, Zimmermann J. Chemical aspects of self-etching enamel-dentin adhesives: a systematic review. *Dent Mater* 2005;21:895–910. [PubMed: 16038969]
24. Carrilho MR, Tay FR, Donnelly AM, Agee KA, Tjäderhane L, Mazzoni A, Breschi L, et al. Host-derived loss of dentin matrix stiffness associated with solubilization of collagen. *J Biomed Mater Res B Appl Biomater* 2009;90:373–380. [PubMed: 19090493]
25. Tay FR, Pashley DH. Guided tissue remineralisation of partially demineralised human dentine. *Biomaterials* 2008;29:1127–1137. [PubMed: 18022228]
26. Xu A, Ma Y, Cölfen H. Biomimetic mineralization. *J Mater Chem* 2007;17:415–449.
27. Gower LB. Biomimetic model systems for investigating the amorphous precursor pathway and its role in biomineralization. *Chem Rev* 2008;108:4551–4627. [PubMed: 19006398]
28. Chesnick IE, Mason JT, Giuseppetti AA, Eidelman N, Potter K. Magnetic resonance microscopy of collagen mineralization. *Biophys J* 2008;95:2017–2026. [PubMed: 18487295]
29. Doi Y, Eanes ED. Transmission electron microscopic study of calcium phosphate formation in supersaturated solutions seeded with apatite. *Calcif Tissue Int* 1984;36:39–47. [PubMed: 6423234]
30. Wang L, Nancollas GH. Pathways to biomineralization and biodemineralization of calcium phosphates: the thermodynamic and kinetic controls. *Dalton Trans* 2009;15:2665–2672. [PubMed: 19333487]
31. Song RQ, Cölfen H, Xu AW, Hartmann J, Antonietti M. Polyelectrolyte-directed nanoparticle aggregation: systematic morphogenesis of calcium carbonate by nonclassical crystallization. *ACS Nano*. 2009 Epub ahead of print.

32. Gu LS, Huffman BP, Arola DD, Kim YK, Mai S, Elsalanty ME, Ling JQ, et al. Changes in stiffness of resin-infiltrated demineralized dentin after remineralization by a bottom-up biomimetic approach. *Acta Biomater* 2010;6:1453–1461. [PubMed: 19887126]
33. Tay FR, Pashley DH. Biomimetic remineralization of resin-bonded acid-etched dentin. *J Dent Res* 2009;88:719–724. [PubMed: 19734458]
34. Mai S, Kim YK, Toledano M, Breschi L, Ling JQ, Pashley DH, Tay FR. Phosphoric acid esters cannot replace polyvinylphosphonic acid as phosphoprotein analogs in biomimetic remineralization of resin-bonded dentin. *Dent Mater* 2009;25:1230–1239. [PubMed: 19481792]
35. Kim J, Arola DD, Gu L, Kim YK, Mai S, Liu Y, Pashley DH, Tay FR. Functional biomimetic analogs help remineralize apatite-depleted demineralized resin-infiltrated dentin via a bottom-up approach. *Acta Biomater*. 2010 Epub ahead of print.
35. Mazzoni A, Pashley DH, Tay FR, Gobbi P, Orsini G, Ruggeri A Jr, Carrilho M, et al. Immunohistochemical identification of MMP-2 and MMP-9 in human dentin: correlative FEI-SEM/TEM analysis. *J Biomed Mater Res A* 2009;88:697–703. [PubMed: 18335530]
36. Meyer JL, Eanes ED. A thermodynamic analysis of the secondary transition in the spontaneous precipitation of calcium phosphate. *Calcif Tissue Res* 1978;25:209–216. [PubMed: 30523]
37. Tay FR, Pashley DH, Yoshiyama M. Two modes of nanoleakage expression in single-step adhesives. *J Dent Res* 2002;81:472–476. [PubMed: 12161459]
38. Pashley DH, Carvalho RM, Sano H, Nakajima M, Yoshiyama M, Shono Y, et al. The microtensile bond test: a review. *J Adhes Dent* 1999;1:299–309. [PubMed: 11725659]
39. Deshpande AS, Beniash E. Bioinspired synthesis of mineralized collagen fibrils. *Cryst Growth Des* 2008;8:3084–3090.
40. Hosaka K, Nishitani Y, Tagami J, Yoshiyama M, Brackett WW, Agee KA, Tay FR, et al. Durability of resin-dentin bonds to water- vs. ethanol-saturated dentin. *J Dent Res* 2009;88:146–151. [PubMed: 19278986]
41. Tay FR, Pashley DH, Kapur RR, Carrilho MR, Hur YB, Garrett LV, et al. Bonding BisGMA to dentin - a proof of concept for hydrophobic dentin bonding. *J Dent Res* 2007;86:1034–1039. [PubMed: 17959892]
42. Kim J, Gu L, Breschi L, Tjäderhane L, Choi KK, Pashley DH, Tay FR. Implication of ethanol wet bonding in hybrid layer remineralization. *J Dent Res*. in press.
43. Wolf SE, Leiterer J, Kappl M, Emmerling F, Tremel W. Early homogenous amorphous precursor stages of calcium carbonate and subsequent crystal growth in levitated droplets. *J Am Chem Soc* 2008;130:12342–12347. [PubMed: 18717561]
44. Spencer P, Wang Y. Adhesive phase separation at the dentin interface under wet bonding conditions. *J Biomed Mater Res* 2002;62:447–456. [PubMed: 12209931]
45. Gunasekaran G, Natarajan R, Muralidharan VS, Palaniswamy N, Rao Appa. Inhibition by phosphonic acids - an overview. *Anti-Corros Method M* 1997;44:248–259.

Control - degradation
of hybrid layer after aging
in SBF for 12 months



Experimental -after
12 months of biomimetic
remineralization



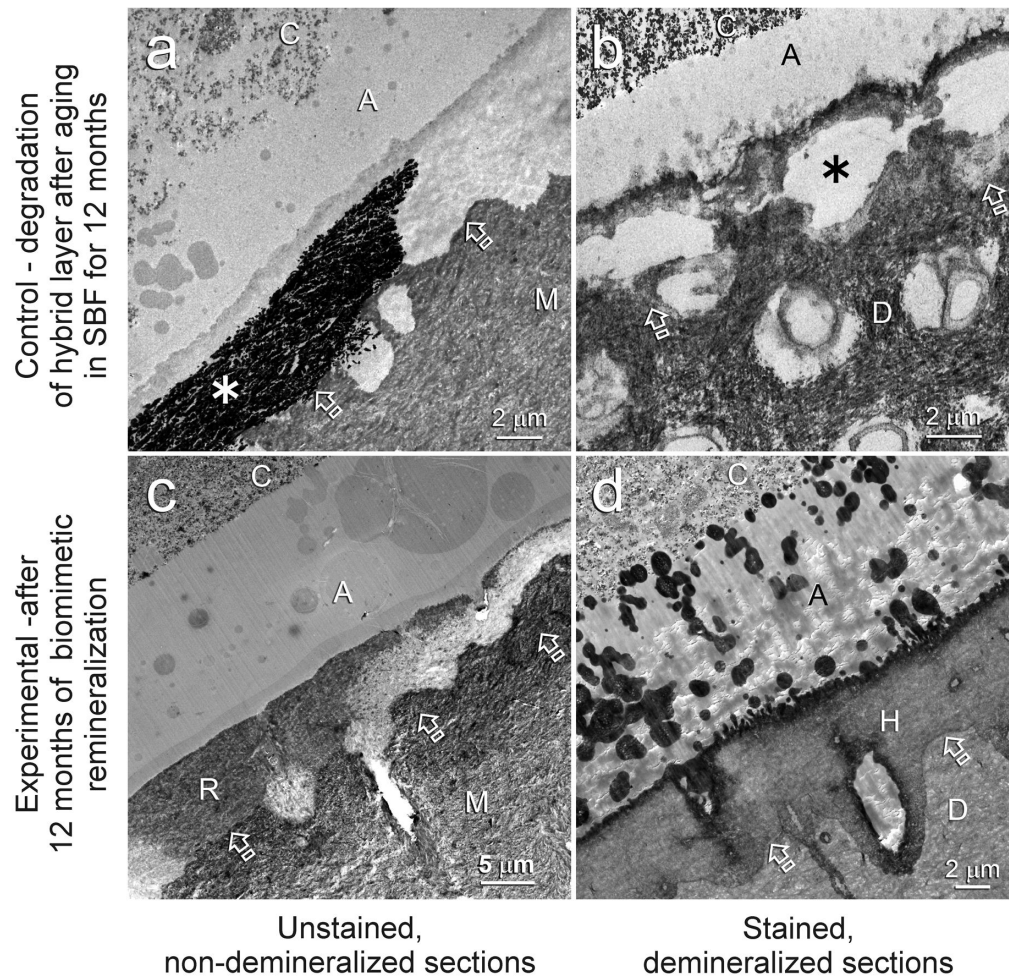
Unstained,
non-demineralized sections

Stained,
demineralized sections

Fig. 1.

TEM images of representative One-Step bonded hybrid layers after 12 months of aging in the control simulated body fluid medium (**a** and **b**) or in the biomimetic remineralization medium (**c** and **d**). Generic abbreviations: A: adhesive; M: mineralized dentin; D: laboratory demineralized dentin; Open arrows: base of hybrid layer. **a.** Unstained, non-demineralized, silver-impregnated section showing extensive silver uptake within the hybrid layer (asterisk). A silver-impregnated water channel (arrow) could also be seen in the adhesive. **b.** Stained, demineralized section showing degradation of the collagen network predominantly along the bottom half of the hybrid layer (asterisk), corresponding to the region of silver uptake in Fig. 1a. Only resin tags (T) remained in this region. **c.** Unstained, non-demineralized section showing remineralization within the hybrid layer (R), the location of

which corresponds roughly to the silver-impregnated fluid-filled spaces (Fig. 1a) and the site of degradation (Fig. 1b) in the control, non-remineralized specimens. **d.** *In-situ* demineralized, stained section of a remineralized hybrid layer showing normal dentin (i.e. absence of collagen degradation) within the hybrid layer (H). C: resin composite.



Control - degradation
of hybrid layer after aging
in SBF for 12 months

Experimental - after
12 months of biomimetic
remineralization

Unstained,
non-demineralized sections

Stained,
demineralized sections

Fig. 2.

TEM images of representative Single Bond bonded hybrid layers after 12 months of aging in the control simulated body fluid medium (**a** and **b**) or in the biomimetic remineralization medium (**c** and **d**). Generic abbreviations: A: adhesive; M: mineralized dentin; D: laboratory demineralized dentin; C: resin composite; Open arrows: base of hybrid layer. **a.** Unstained, non-demineralized, silver-impregnated section showing extensive silver deposition within parts of the hybrid layer (asterisk). **b.** Stained, demineralized section showing degradation predominantly along the bottom half of the hybrid layer (asterisk). **c.** Unstained, non-demineralized section showing remineralization within the hybrid layer (R), the location of which corresponds roughly to the silver-impregnated fluid-filled spaces (Fig. 2a) and the site of degradation (Fig. 2b) in the control, non-remineralized specimens. **d.** *In-situ* demineralized, stained section of a remineralized hybrid layer showing the presence of normal dentin matrix (i.e. absence of collagen matrix degradation) within the hybrid layer (H).

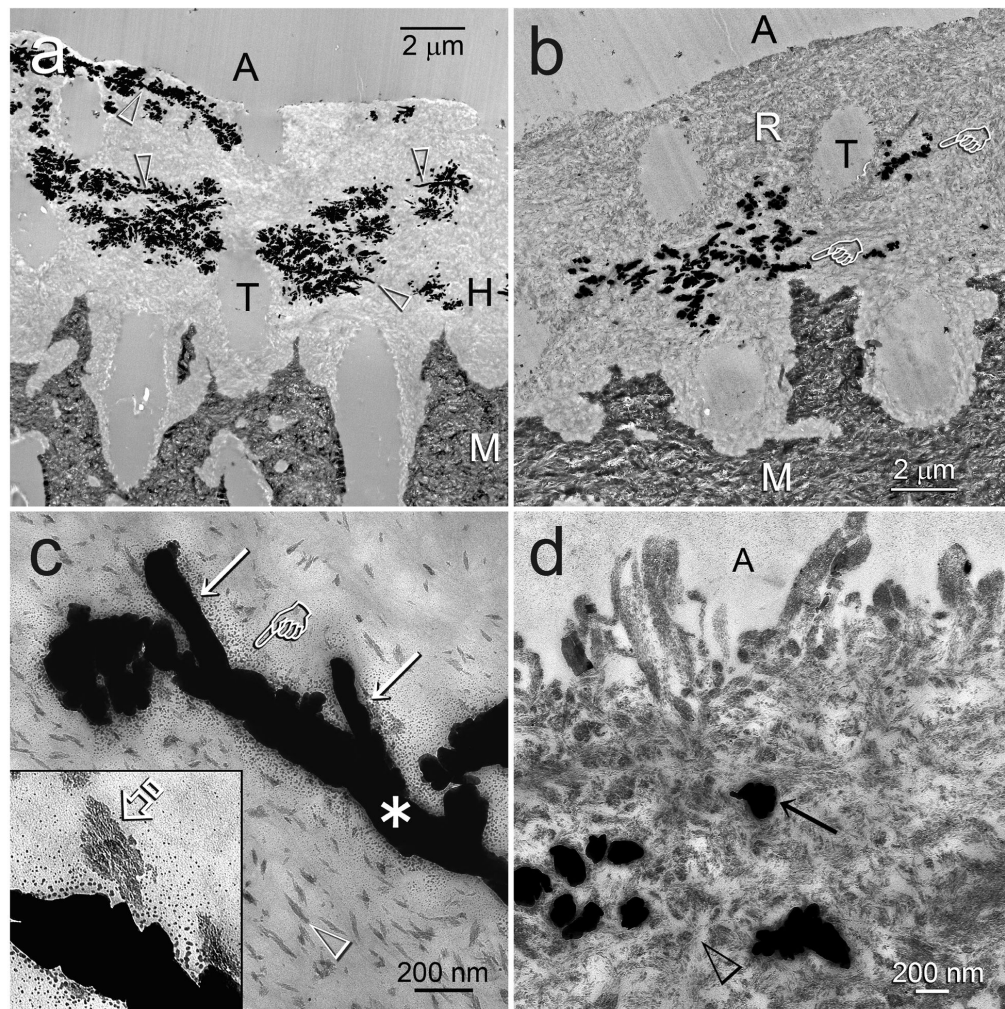


Fig. 3. TEM images of silver-impregnated, unstained, non-demineralized sections of One-Step bonded acid-etched dentin illustrating the changes in silver tracer distribution within hybrid layers after biomimetic remineralization. Generic abbreviations: A: adhesive; M: mineralized dentin. T: dentinal tubule. **a.** Baseline specimen that had not been remineralized. Extensive silver deposits within the hybrid layer (H) exhibited a reticular pattern, with ramifications branching off from wider silver-filled micro-branches of the dentinal tubule (open arrowheads). **b.** An early stage of biomimetic remineralization showing reduction in silver tracer uptake within the partially-remineralized hybrid layer (R), compared to the non-remineralized baseline specimen in Fig. 3a. The reticular pattern of silver deposits was absent and only the micro-branches of the tubules were impregnated with silver (pointers). **c.** High magnification of a 200 nm wide, silver-impregnated micro-branch (asterisk) of the dentinal tubule that ramifies into 100 nm wide side branches (arrows). Small silver grains with a gradient of dimensions (pointer) extended from the water-filled channel into the resin-infiltrated collagen matrix. Collagen fibrils were partially-remineralized (open arrowhead). Inset: Higher magnification of intrafibrillar remineralization in a collagen fibril with nanocrystals (open arrow) deposited along the microfibrillar strands of the fibril. **d.** A more advanced stage of biomimetic remineralization showing predominant intrafibrillar remineralization of the collagen fibrils. The interfibrillar spaces (open arrowhead) were filled with polymerized adhesive resin and contained minimal nanocrystals and no silver

deposits. The 200 nm diameter silver deposits (arrow) are cross sections of the water-filled channels depicted by the asterisk in Fig. 3c.

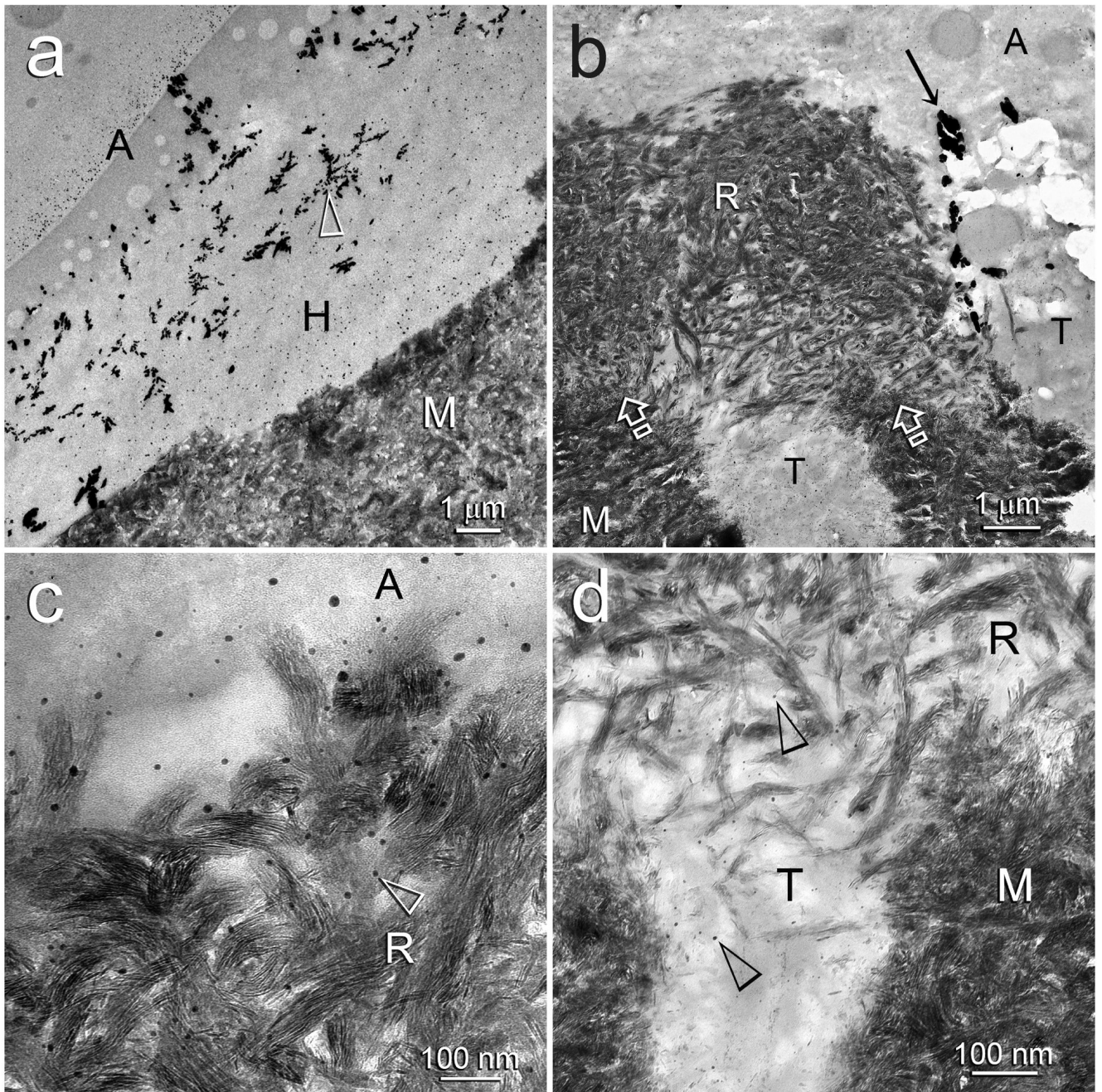


Fig. 4. TEM images of silver-impregnated, unstained, non-demineralized sections of Single Bond bonded acid-etched dentin illustrating the changes in silver tracer distribution within hybrid layers after biomimetic remineralization. Generic abbreviations: A: adhesive; M: mineralized dentin; H: original non-remineralized hybrid layer; T: dentinal tubule. **a.** Baseline specimen showing the reticular pattern (open arrowhead) of silver tracer as described in Fig. 3a. The globules in the adhesive are phase separations of polyalkenoic acid in the Single Bond adhesive. **b.** An advanced stage of biomimetic remineralization similar to that depicted in Fig. 2c. Silver-impregnated water channels were not evident in the heavily remineralized hybrid layer (R). However, silver deposits (arrow) could be seen within a

dentinal tubule that contained a resin tag. **c.** High magnification of the surface of the remineralized hybrid layer (R). Although gross, silver-filled water channels were absent, isolated silver grains (open arrowhead) could be identified within the adhesive and interfibrillar spaces. **d.** High magnification of the base of the remineralized hybrid layer (R) showing isolated silver grains (open arrowheads) within the polymerized adhesive resin.

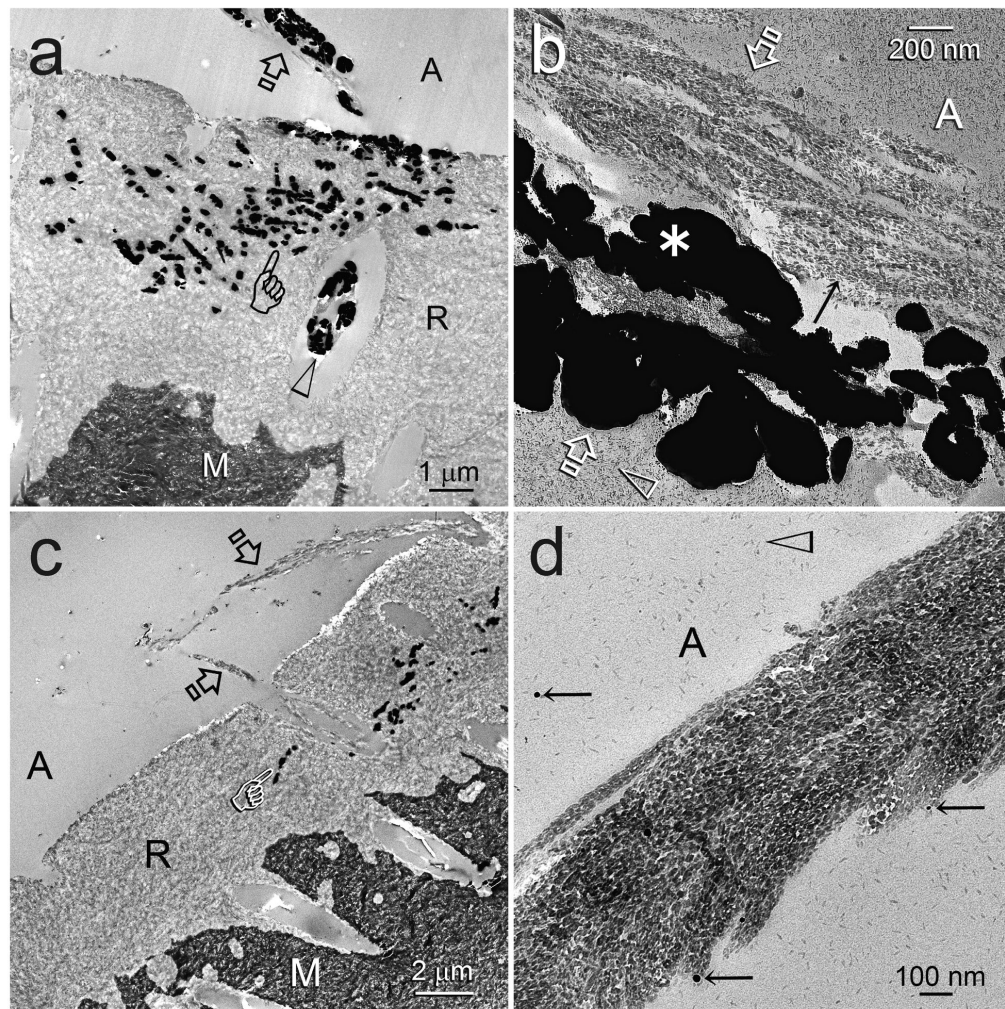


Fig. 5. TEM images of silver-impregnated, unstained, non-demineralized sections of One-Step bonded acid-etched dentin illustrating the reduction of bulk free water from water channels entrapped within the adhesive layer by nanocrystals derived from biomimetic remineralization. Generic abbreviations: A: adhesive; R: remineralized hybrid layer; M: mineralized dentin. **a.** An early stage of remineralization in which bulk water from some of the micro-branches of the dentinal tubules were still retained within the hybrid layer (pointer). Silver tracer also extended from a dentinal tubule (open arrowhead) into an obliquely-oriented water-filled channel (open arrow) in the adhesive. **b.** High magnification of the water-filled channel from Fig. 5a (between open arrows), showing both bulk silver deposits (asterisk) and nanocrystals derived from biomimetic remineralization (black arrow). The resin matrix adjacent to the water-filled channel also contained smaller nanocrystals (open arrowhead). **c.** A more advanced stage of remineralization with marked reduction, albeit incomplete, of bulk water (i.e. silver uptake) within the micro-branches of the dentinal tubules (pointer) in the remineralized hybrid layer. No silver deposits were seen in the remineralized water-filled channels (open arrows). **d.** High magnification of a remineralized water-filled channel from Fig. 5c showing complete displacement of bulk water within the channel by nanocrystals. Only sparse, isolated silver grains (arrows) could be identified within the unfilled resin matrix, which also contain nanocrystals derived from biomimetic remineralization (open arrowhead).

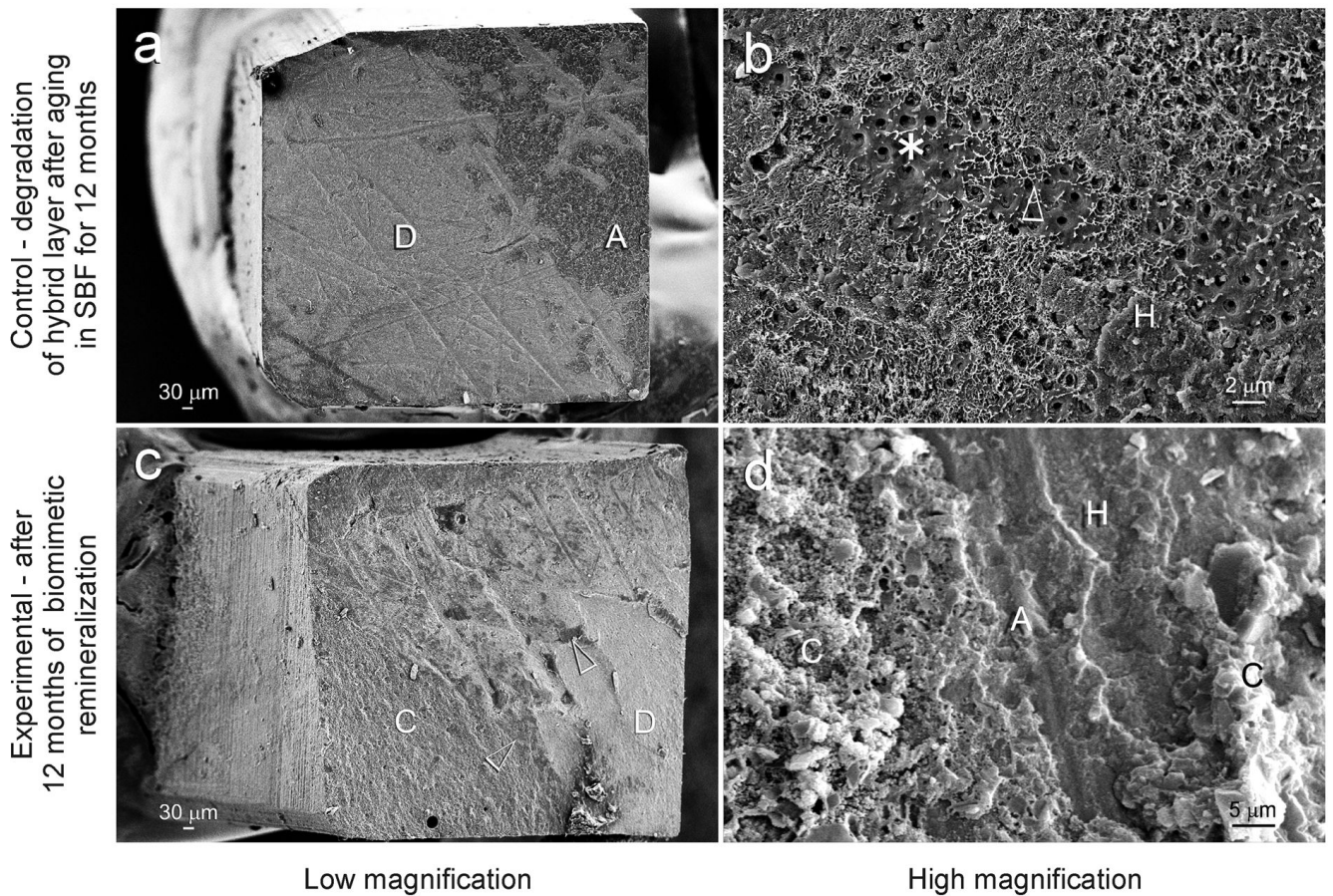


Fig. 6. SEM images of the dentin side of separated beams after they were stressed to failure by tensile testing. The images selected were taken from resin-dentin beams that had been aged for 12 months in the control simulated body fluid medium (**a** and **b**) or in the biomimetic remineralization medium (**c** and **d**). The selected beams were representative of the mean bond strength from that group at 12 months. **a.** A separated beam in the One-Step control group (tensile bond strength = 19.6 MPa) showing a mixed failure mode with adhesive failure in dentin (D) and cohesive failure within the adhesive (A). **b.** High magnification of the dentin part of the beam in Fig. 6a showing part of the hybrid layer (H) and denuded collagen fibrils (open arrowhead) at the base of the fractured hybrid layer. there are regions in which the collagen matrix was completely absent (asterisk), exposing the mineralized dentin base. **c.** A separated beam in the One-Step remineralized group (tensile bond strength = 35.8 MPa) showing a different type of mixed failure with cohesive failure in the composite (C), adhesive (open arrowheads) and along the dentin surface (D). **d.** High magnification of Fig. 6c showing the fractured composite (C), fractured adhesive (A) and the surface of the hybrid layer (H).

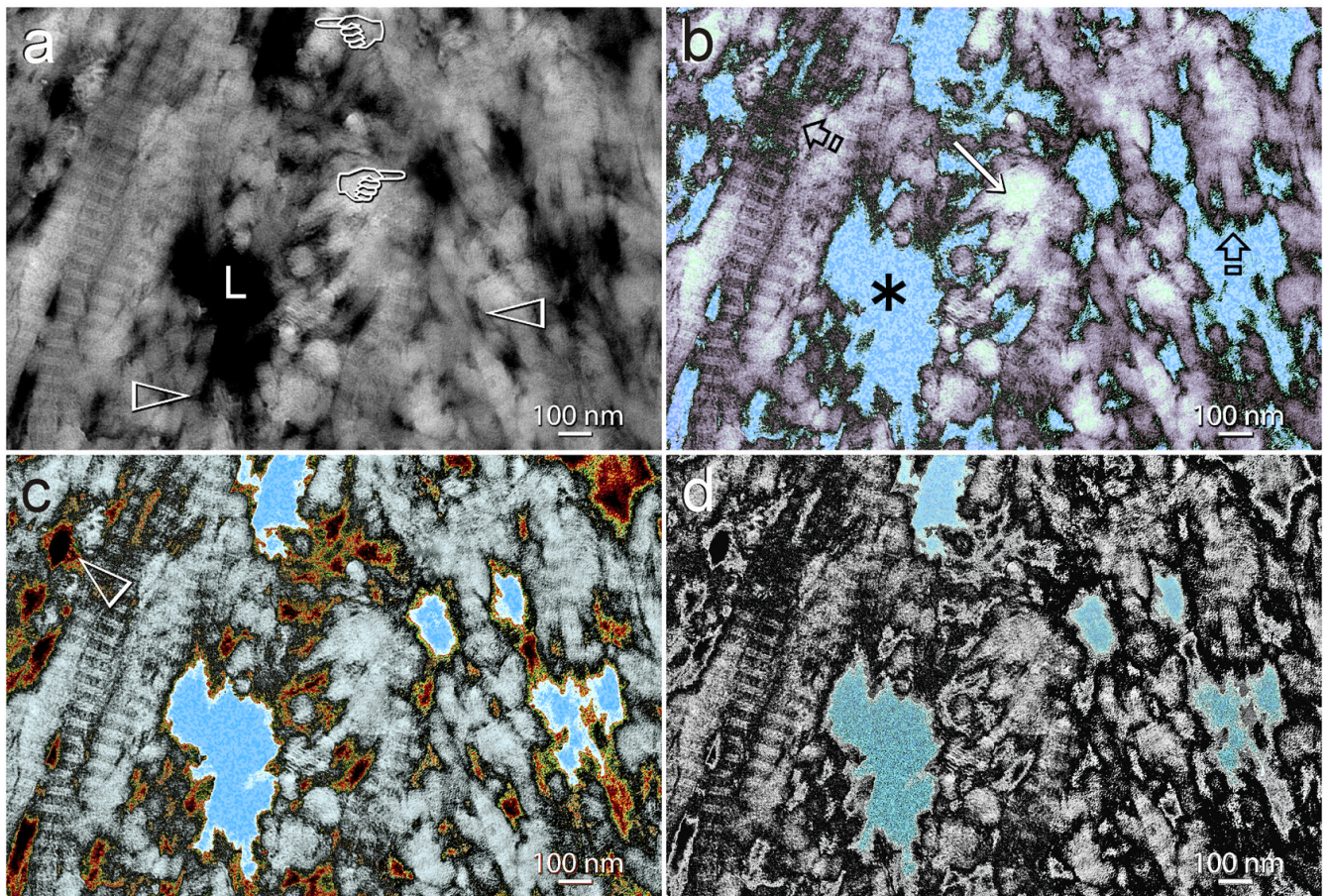


Fig. 7.

A schematic portraying the progressive dehydration of a water-rich, incompletely resin-infiltrated collagen matrix as a result of biomimetic remineralization. **a.** An unmodified, negative-stained demineralized collagen matrix showing a micro-branch of the dentinal tubule (L) that ramifies into terminal branches (pointers) that communicate with the interfibrillar spaces (open arrowheads) of collagen fibrils. **b.** Bulk water-filled spaces within the water-rich regions of non-remineralized hybrid layers were identified with silver tracers, as illustrated by the reticular pattern of silver deposits in Figs 3a and 4a. The free water is shown in blue (asterisk). Collagen fibrils may be sparsely coated by adhesive resin (white regions, identified by open arrows) but the resin does not infiltrate the intrafibrillar compartments of those fibrils, which retain both free and bound water after they are demineralized (arrow). **c.** Biomimetic phosphate-containing polyanionic acid that binds non-specifically to the collagen fibrils acts as templating molecules for guiding the polycarboxylic acid-sequestered amorphous calcium phosphate nanoprecursors (orange color; open arrowhead) to penetrate the intrafibrillar compartments of the collagen fibrils. Free water is displaced from the fibrils as intrafibrillar mineral nanophases are deposited. Dehydration may also occur as nanocrystals are deposited within interfibrillar spaces that are not occupied by resin, as well as from very small water-filled terminal branches of the dentinal tubule. **d.** As the larger micro-branches of the dentinal tubules are unlikely to be completely occluded by nanocrystals, free water may remain within these channels. This gives rise to the appearance of larger silver tracer deposits in the partially-remineralized hybrid layers (see Figs. 3b, 5a).

Table I

Changes in tensile bond strengths with aging of adhesive resin-bonded dentin

Adhesive ^a	Aging period	Control group (MPa) ^b [n = 40 beams]	Remineralized group (MPa) ^b [n = 40 beams]
One-Step	Baseline	37.0 ± 6.2 ^{a,1}	39.2 ± 6.9 ^{A,1}
	1 month	37.8 ± 6.4 ^{a,1}	38.8 ± 5.9 ^{A,1}
	2 months	35.0 ± 5.7 ^{a,1}	40.8 ± 6.9 ^{A,2}
	3 months	33.0 ± 6.3 ^{a,1}	38.4 ± 7.1 ^{A,2}
	6 months	26.9 ± 7.3 ^{b,1}	41.3 ± 8.1 ^{A,2}
	12 months	20.8 ± 4.7 ^{c,1}	37.7 ± 4.9 ^{A,2}
	Single Bond	Baseline	39.8 ± 6.0 ^{a,1}
1 month		40.8 ± 5.6 ^{a,1}	39.8 ± 5.1 ^{A,1}
2 months		39.4 ± 6.7 ^{ab,1}	41.2 ± 7.6 ^{A,1}
3 months		35.4 ± 8.5 ^{bc,1}	40.8 ± 8.8 ^{A,2}
6 months		32.3 ± 6.7 ^{c,1}	40.7 ± 9.7 ^{A,2}
12 months		23.5 ± 4.1 ^{d,1}	38.2 ± 6.0 ^{A,2}

^aData from each adhesive were analyzed separately^bValues are means ± standard deviations. For each column, data followed by the same letter superscripts are not statistically significant ($p > 0.05$). For each row, data followed by the same numerical superscripts are not statistically significant ($p > 0.05$)